2013-09-23

Microwave plasma based single step method for free standing graphene synthesis at atmospheric conditions

Tatarova, E.; Henriques, J.; Luhrs, C.C.; Dias, A.; Phillps, J.; Abrashev, M.V.; Ferreira, C. M.

Journal Name: Applied Physics Letters; Journal Volume: 103; Journal Issue: 13; Other Information: (c) 2013 AIP Publishing LLC; Country of input: International Atomic Energy Agency (IAEA)
http://hdl.handle.net/10945/57251

Microwave plasma based single step method for free standing graphene synthesis at atmospheric conditions

E. Tatarova,[1,a)] J. Henriques,[1] C. C. Luhrs,[2] A. Dias,[1] J. Phillips,[2] M. V. Abrashev,[3] and C. M. Ferreira[1]
[1]*Institute of Plasmas and Nuclear Fusion, Instituto Superior Técnico, Technical University of Lisbon, Portugal*
[2]*Department of Mechanical and Aerospace Engineering, Naval Postgraduate School, Monterey, California 93943, USA*
[3]*Faculty of Physics, Sofia University, 1164 Sofia, Bulgaria*

(Received 15 July 2013; accepted 9 September 2013; published online 24 September 2013)

Microwave atmospheric pressure plasmas driven by surface waves were used to synthesize graphene sheets from vaporized ethanol molecules carried through argon plasma. In the plasma, ethanol decomposes creating carbon atoms that form nanostructures in the outlet plasma stream, where external cooling/heating was applied. It was found that the outlet gas stream temperature plays an important role in the nucleation processes and the structural quality of the produced nanostructures. The synthesis of few layers (from one to five) graphene has been confirmed by high-resolution transmission electron microscopy. Raman spectral studies were conducted to determine the ratio of the 2D to G peaks (>2). Disorder D-peak to G-peak intensity ratio decreases when outlet gas stream temperature decreases. © *2013 AIP Publishing LLC*. [http://dx.doi.org/10.1063/1.4822178]

Graphene, an atomically thin sheet of carbon atoms tightly packed in a two-dimensional (2D) honeycomb lattice, possesses many extraordinary properties and shows enormous potential as an energy storage material.[1–4] Thus, it is of primary importance to develop efficient and solid processing methods to synthesize graphene with controlled structural quality and at reasonable cost. Methods developed thus far rely on three-dimensional crystals or substrates to obtain 2D graphene. These techniques include the micromechanical cleavage of graphite, the chemical reduction of exfoliated graphite oxide, the vacuum graphitization of silicon carbide substrates, and the growth of graphene on metal substrates.[2] Graphene of the highest quality can be obtained by mechanically exfoliating highly oriented pyrolytic graphite but this approach cannot be scaled up for commercial applications. This has driven a search for an alternative technique capable of obtaining high yields of clean and highly ordered/disordered graphene sheets. Large area graphene has been created by chemical vapor deposition (CVD) but this method is dependent on the quality of an underlying polycrystalline metallic film. The synthesis of graphene by CVD requires multiple processing steps, such as wet-etching and micro-fabrication, to obtain transferable sheets.[2,5–10] Moreover, all the techniques mentioned above do not readily yield self standing graphene.

The unique chemically active plasma environment provides suitable conditions to create extraordinary synthetic pathways and unique structures.[4] Many applications exploit the ability of plasmas to break down complex molecules considering that plasma systems provide simultaneously high temperatures and a highly reactive environment. For example, plasma enhanced chemical vapor deposition (PECVD) is frequently employed.[9–12] These methods, as a rule, require substrates and low-pressure environments (below 10 Torr) to obtain carbon nanostructures. The synthesis and growth of these structures proceed via surface reactions and hence are dependent on the substrate conditions.

Recently, there has been increased interest in using plasma techniques for creating particulate materials homogeneously. Particulate materials created using novel plasma techniques include metal nanoparticles,[13] supported metal catalysts,[14] nano-oxide particles, core-shell nanoparticles, spherical ceramic particles of controlled size, carbon nanotubes,[15] spherical boron nitride, carbon-graphite-coated nanoparticles, and graphene. One technique, known as aerosol-through-plasma (A-T-P) technique[16–18] is particularly suited for relatively easy scale-up as it generally operates at atmospheric pressure. This method has also been applied to synthesize substrate free graphene sheets.[18,19] The quality of the graphene sheets has been controlled by the amount of precursors in the feeding gas stream, the microwave power, and the flux of background gas used. However, the existing sharp drop of the gas temperature in the plasma outlet gas stream is to be noted. Therefore, the thermodynamic conditions for nucleation and growth processes in this zone strongly change due to the gas temperature spatial gradients.[20–23] For this reason, tuning of the plasma and its afterglow properties is of crucial importance to establish a solid plasma-based method, with a rigid parametric control on the graphene synthesis processes, in order to take into account particular requirements concerning its structural quality.

In the present work, microwave atmospheric plasmas driven by surface waves have been used to generate various carbon nanostructures, including graphene sheets and nanoparticles. The method is based on sending vaporized ethanol molecules through a microwave argon plasma environment, where decomposition of ethanol molecules takes place and carbon atoms are created. These carbon atoms agglomerate subsequently in the outlet plasma stream to form nanostructures. Since the temperature of the outlet plasma stream is a

[a)]Author to whom correspondence should be addressed. Electronic mail: e.tatarova@ist.utl.pt

key parameter for the nucleation process, externally forced cooling/heating has been applied to adjust the temperature spatial profile in the nucleation zone of the plasma reactor. In fact, forced change of thermal conditions in the plasma afterglow and following outlet gas stream results in dramatic changes in the structure of the particulate material produced.

A surfatron-based setup is used to create a surface wave induced microwave plasma at atmospheric pressure conditions.[24] The microwave power is provided by a 2.45 GHz generator (Sairem), whose output power was varied from 400 to 900 W. The generator is connected to a waveguide (WR-340) system, which includes an isolator, directional couplers, a 3-stub tuner and a waveguide surfatron as the field applicator. The system is terminated by a movable short-circuit. The discharge takes place inside a quartz tube with internal and external radii of 7.5 mm and 9 mm, respectively, which is inserted vertically and perpendicularly to the waveguide wider wall. A second quartz tube is used to introduce the vaporized precursor, i.e., ethanol molecules, in the discharge zone. The background argon gas is injected into the discharge tube at flow rates (Φ) varying from 250 to 2000 sccm under laminar gas flow conditions. The precursor partial flux (Φ_{pr}) varies in the range 0.5 to 3.5 sccm. Vaporization is performed at room temperature by passing argon gas through a porous filter, composed of bonded grains of quartz glass immersed in the precursor liquid inside a tank. The total flow passing through the discharge consists of the direct argon flow passing through the large quartz tube plus the combined flows of the argon bubbling in the precursor liquid and the vaporized precursor, passing though the second quartz tube. Gas flow rates are controlled by a MKS247 Readout coupled to two MKS flow meters. The outlet gas stream temperature was actively controlled by a cryostat system. The cooling/heating fluid circulates, with a constant flow rate, between the cryostat and a tubular heat exchanger as shown in Fig. 1. The heat exchanger consists of an external pyrex tube, with internal and external radii of 36 and 42 mm, concentrically aligned with the quartz tube where the discharge takes place; the wall of the quartz tube is the heat transfer surface. The heat exchanger (length 20 cm) is placed immediately after the end of the discharge zone, whose length is about 10–12 cm as seen in Fig. 1.The nanostructures were captured by a membrane filter system coupled to an Edwards BS2212 two-stage vacuum pump.

In order to understand the impact of external cooling/heating on the growth of carbon structures, it is essential to map the plasma structure. The active microwave plasma region of the reactor considered (Fig. 1) is composed of two zones. The first one is the surface wave sustained discharge zone, including the zone inside the launcher and the extended "hot" plasma zone outside the launcher. Here, the surface wave power is absorbed by plasma electrons, which transfer this power to heavy particles via elastic and inelastic collisions, high gas temperatures (up to 3000 K) being achieved. The gas temperature keeps nearly constant in the discharge zone when moving away from the launcher (up to about 10 cm) and then drops sharply in the "near" ($\sim$13 cm) afterglow plasma zone.[23] These two regions ($\sim$13 cm) form the active plasma zone, where the ethanol molecules are thermally decomposed into simple atoms and molecules (C, H, H_2, C_2, CO, CO_2) due to the high temperature. The next final zone is the "nucleation and growth zone" (see Fig. 1) where kinetic processes of nucleation and growth take place. It can be expected that the temperature profile in the nucleation zone can strongly impact the final product structure. For example, too long a residence time in this zone might result in too much growth, thus allowing graphene particles to agglomerate and form graphite. Indeed, the results obtained demonstrate that the type of nanostructures created strongly depends on external cooling/heating applied.

To monitor the ethanol molecules decomposition processes and identify species of interest, and determine as well the gas temperature in the discharge "hot" zone, plasma emission spectroscopy has been applied. In fact, optical emission spectroscopy permits to identify the active species present in the plasma during the synthesis of the carbon nanostructures in the outlet gas stream. To this end, the plasma radiation was collected by a quartz optical fiber coupled to a Jobin-Yvon Spex 1250 spectrometer equipped with a cryogenic, back illuminated UV sensitive CCD camera. The emission of $C_2(A^3\Pi_g \rightarrow X'^3\Pi_u)$ (Swan system, between 4500–5700 Å), OH ($A^2\Sigma^+$, $\upsilon = 0 \rightarrow X^2\Pi_i$, $\upsilon' = 0$) (3000–3200 Å) bands has been detected. The detected emission of carbon atoms at 2479 Å, the main species of interest for carbon nanostructure synthesis, is to be noticed. An estimation of the gas temperature was obtained from measurements of the rotational OH ($A^2\Sigma^+$, $\upsilon = 0 \rightarrow X^2\Pi_i$, $\upsilon' = 0$) (3000–3200 Å) spectra assuming local thermodynamic equilibrium between rotational and translational degrees of freedom.[20–23] The gas temperature measured in this way at $z = 2$ cm from the launcher (nearly at the middle of the "hot" plasma zone) was found to increase linearly from 1300 K to 2000 K when microwave power increases from 300 to 900 W. It should be mentioned that this temperature is associated with the axial part of the "hot" plasma column as far as the radiation collected originates mainly from this region.

A parametric study has been performed to determine the optimal range of discharge operational conditions, in terms of precursor and argon gas fluxes, for the synthesis of planar carbon nanostructures. The results show that such structures are synthesized at 0.6 sccm partial ethanol flux and 250 sccm argon gas flux. Aiming at planar nanostructures, all further experiments have been done fixing the above values of the fluxes and changing only two parameters, *viz*., microwave power and wall temperature (T_{wall}) of the outlet plasma and gas stream. Furthermore, by externally forced cooling/heating of the outlet plasma stream, it was found that the nucleation processes can be controlled in a way to create nanostructures with different shapes, i.e., particles or sheets.

The evolution in the shape of the synthesized nanostructures when externally forced cooling/heating is applied is shown in Fig. 2. Nearly spherical particles with diameters in the range of 10 to 25 nm (usually referred to in the literature as fullerene soot[25]) are formed at low (0 °C–10 °C) wall temperatures (Fig. 2). At the temperature of 18 °C there is a mix of particles and sheets, while at 60 °C extended sheets are the only nanostructures present. It should be recalled that the reduction of the Gibbs free energy of a saturated environment (gas + solid phase) is a driving force for both nucleation and growth.[26] This reduction is proportional to the gas

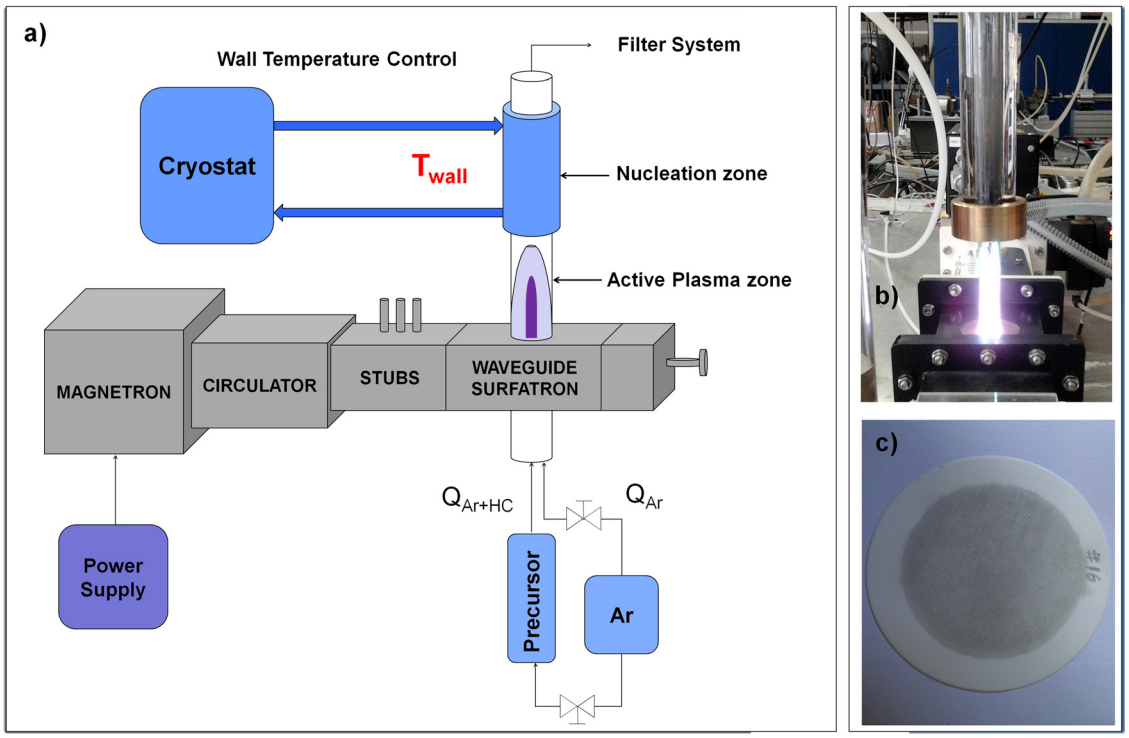

FIG. 1. Experimental setup (a); picture of the plasma column and heat exchanger (b); nylon filter with 2 mg of graphene (c).

temperature. Lower gas temperatures as well as large amounts of precursors foster supersaturation conditions in the environment (gas + solid phase) and thus promote synthesis of plenty of multiple nuclei, while higher temperatures (and lower precursor amounts) favor the appearance of less nuclei and, consequently, a deviation from supersaturation conditions.

The Raman spectrum and low magnification TEM images of the synthesized carbon sheets at 900 W microwave power and 100 °C are shown in Fig. 3. Graphene sheets collected on the filters (the filter with graphene is shown in Fig. 1(c)) were freely suspended on the lacey carbon grids for electron microscopy analysis. A 200 kV JEOL 2010 transmission electron microscope has been used to characterize the graphene sheets. Note that the graphene sheets were found to be stable at atmospheric conditions.

As seen in this image, there are both homogeneous and less transparent areas in the synthesized sheet, as large as several hundred nm. The less transparent areas can be attributed to the folding and overlapping of single sheets or the overlapping of multiple sheets, while the dark areas are a result of crumpled regions. It can be expected that homogeneous and featureless zones likely correspond to single or few layers graphene sheets. Further evidence for this was found using Raman spectroscopy.

In order to perform Raman spectroscopy, the synthesized nanostructures were freely suspended on a glass substrate and the Raman spectra from different regions on the substrate were obtained using a LabRAM HR Visible (Horiba JobinYvon) Raman spectrometer at 633 nm, with 5 cm^{-1} spectral resolution and a laser spot size of 2 μm. Measurements were performed with a laser power $P_l = 0.054$ mW to avoid overheating. A typical Raman spectrum is shown in Figure 3. As seen in this figure, the sheets exhibit a sharp 2D peak at about 2661 cm^{-1} due to the second order process and a G-band peak due to the tangential zone center

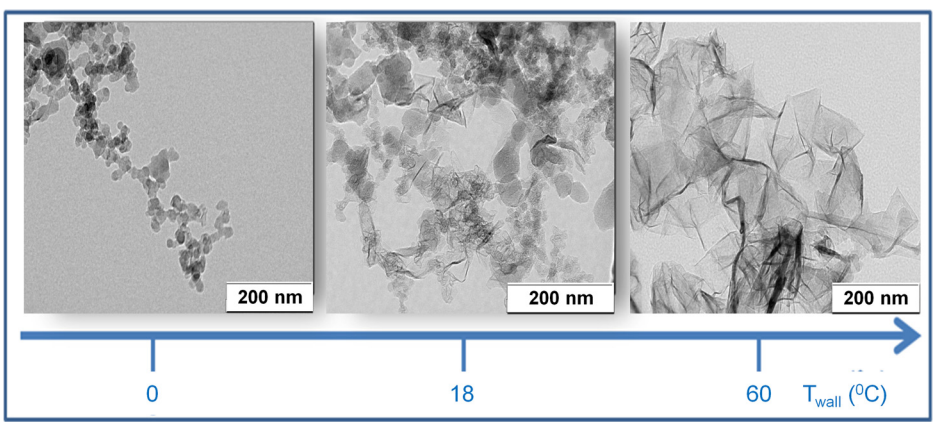

FIG. 2. Evolution in the shape of synthesized structures (TEM images; scale bar is 200 nm) with wall temperature ($P = 500$ W; $\Phi = 250$ sccm; $\Phi_{pr} = 0.6$ sccm).

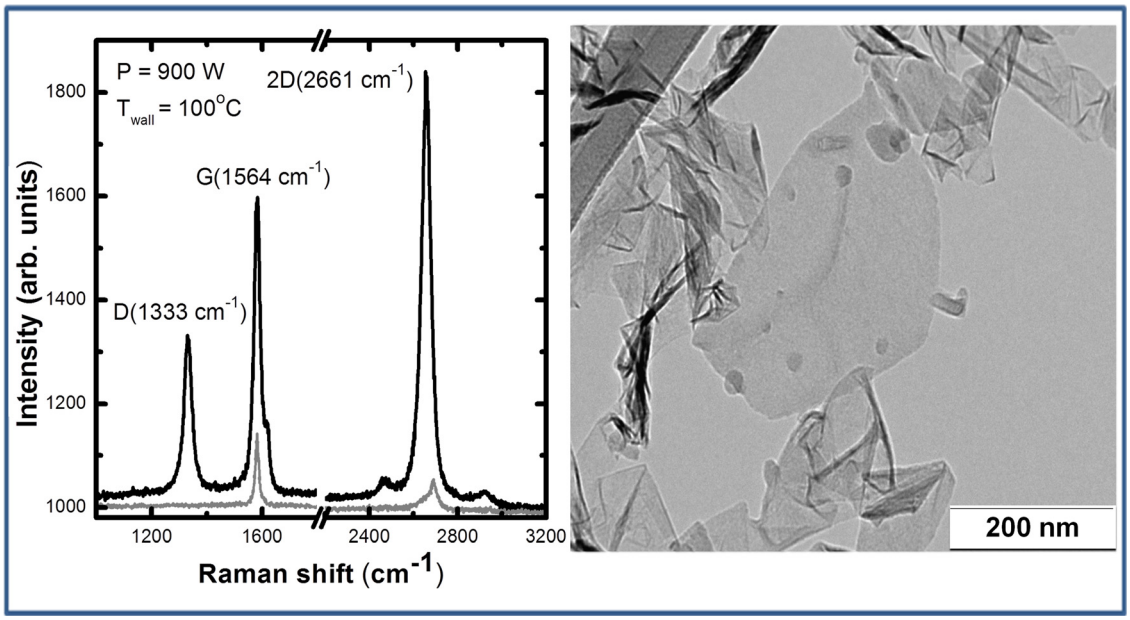

FIG. 3. Typical Raman spectrum and corresponding TEM image of the sheets synthesized at microwave power $P = 900$ W and wall temperature $T_{wall} = 100\,^{\circ}$C. For comparison, the Raman spectrum of graphite powder is also shown with grey line.

mode at 1564 cm^{-1}.[27] This type of Raman spectra has often been associated with graphene and provides strong evidence in support of the fact that the obtained nanosheets are indeed graphene. For comparison, Raman spectra of graphite powder are also shown. As seen, there are significant changes in the shape and intensity of the 2D peak of graphene as compared to the graphite one. The 2D peak of graphite is much less intense, with a rather large full-width at half maximum ($\sim$75 cm^{-1}), while for graphene it is a single sharp peak red shifted in respect to that of graphite. Notably, the G-peaks of graphene and graphite are comparable. The appearance of the D peak at $\sim$1333 cm^{-1} and the small shoulder of the G peak at $\sim$1620 cm^{-1} can be considered as a result of structural disorders in the created sheets and/or edge effects.[27]

The most prominent feature in the Raman spectrum of graphene is the 2D peak, whose position, shape and intensity are frequently used to distinguish between single-layer, bilayer, and multi-layer graphene. Taking into account the ratio between the 2D and G peak integral intensities, which varies between 2–2.6, and the full width at half maximum of the 2D-band ($\sim$45 cm^{-1}) the obtained results can be interpreted as an indication of few layer graphene synthesis. The decrease of the ratio of the disorder D-peak to the G-peak intensities with increasing wall temperature is to be noted.

The graphene nanosheets have been further characterized by high-resolution TEM. This was performed with a Titan ChemiStem (FEI) HRTEM operating at 200 kV. Figure 4(a) shows the HRTEM images of graphene sheets synthesized at 900 W microwave power and wall temperature of 80 °C, freely suspended on the grid. The evident upward curling at the edges of the individual flakes may be due to internal stress in the few-layer graphene; these edges make it possible to evaluate the thicknesses of the sheets. As seen from the images, single (1L) and few (2L–5L) layers graphene sheets can be easily distinguished. Moreover, highly ordered lattice fringes can be observed, indicating that the graphene sheets are well-crystallized. A zoomed image of the areas with single layer graphene (marked region) is shown in Figure 4(b). From the HRTEM images, it can be seen that the interlayer spacing of plasma produced graphene has an average value (3.5 Å) significantly larger than that of graphite (3.35 Å).

In summary, we have demonstrated that the nature of the synthesized carbon nanostructures, in particular of graphene sheets, can be controlled by adjusting the gas temperature spatial profile in the outlet plasma stream where the nucleation and growth processes take place. Our investigation shows that the gas temperature spatial profile plays an important role in the formation of the graphene sheets morphology and in their structural quality. The microwave plasma-based method developed here is a single step method at ambient conditions that does not require transient metals and complex processing conditions. The synthesized graphene sheets are stable and highly ordered. The sheets disorder can be reduced/increased by increasing/decreasing the gas temperature in the outlet plasma stream. This control can

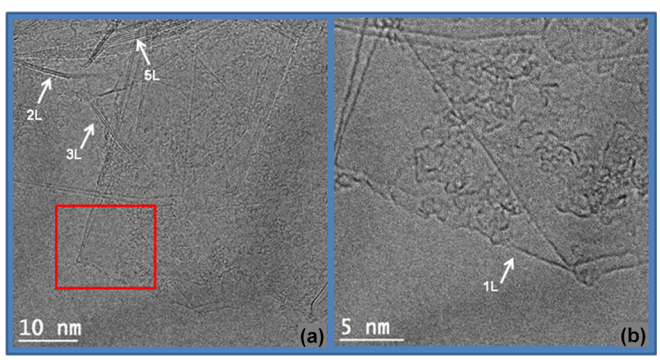

FIG. 4. (a) TEM image of suspended graphene obtained at microwave power of 900 W and wall temperature 80 °C; (b) Raw HRTEM image of the zone marked showing single layer (1L) graphene sheets.

be done by changing the microwave power or/and the externally forced heating of the nucleation zone. The obtained sheets exhibit a structural quality comparable to that of existing graphene materials, but they are synthesized here without the need of metal or crystal substrates. The graphene yield is determined by the area of the nylon filter used. By optimizing the microwave plasma reactor performance, in what concerns the regime of gas flow, i.e., laminar or vortex, type of precursors, discharge geometry (e.g., using large scale discharge configurations[28,29]), along with detailed kinetic modeling of the plasma environment and ethanol decomposition process,[23] well controlled synthesis of carbon atom lattices can be achieved. This approach paves the way towards scalable production of graphene structures for numerous applications. Further investigation is in progress to analyze in detail the electrical and optical properties of the synthesized graphene sheets. The results of such investigations will be reported in the future.

This work was supported by the Portuguese *Fundação para a Ciência e a Tecnologia*, through the research contract PTDC/FIS/108411/2008.

[1]J. C. Meyer, A. K. Geim, M. I. Katsnelson, K. S. Novoselov, T. J. Booth, and S. Roth, Nature Lett. **446**, 60 (2007).
[2]Y. H. Wu, T. Yu, and Z. X. Shen, J. Appl. Phys. **108**, 071301 (2010).
[3]Y. Yurum, A. Taralp, and N. Veziroglu, Int. J. Hydrogen Energy **34**, 3784 (2009).
[4]K. Ostrikov, U. Cvelbar, and A. B. Murphy, J. Phys. D: Appl. Phys. **44**, 174001 (2011).
[5]A. Reina, X. Jia, J. Ho, D. Nezich, H. Son, V. Bulovic, M. S. Dresselhaus, and J. Kong, Nano Lett. **9**, 30 (2009).
[6]W. Gannett, W. Regan, K. Watanabe, T. Taniguchi, M. F. Crommie, and A. Zettl, Appl. Phys. Lett. **98**, 242105 (2011).
[7]S. Garaj, W. Hubbard, and J. A. Golovchenko, Appl. Phys. Lett. **97**, 183103 (2010).
[8]M. Zhu, J. Wang, B. C. Holloway, R. A. Outlaw, X. Zhao, K. Hou, V. Shutthanandan, and D. M. Manos, Carbon **45**, 2229 (2007).
[9]T. Yamada, J. Kim, M. Ishihara, and M. Hasegava, J. Phys. D: Appl. Phys. **46**, 063001 (2013).
[10]S. Vizireanu, S. D. Stoica, C. Luculescu, L. C. Nistor, B. Mitu, and G. Dinescu, Plasma Sources Sci. Technol. **19**, 034016 (2010).
[11]G. Nandamuri, S. Roumimov, and R. Solanki, Appl. Phys. Lett. **96**, 154101 (2010).
[12]K. S. Hazra, J. Rafiee, M. A. Rafiee, A. Mathur, S. S. Roy, J. McLauhglin, N. Koratcar, and D. S. Misra, Nanotechnology **22**, 025704 (2011).
[13]C. H. Chou and J. Phillips, J. Mater. Res. **7**, 2107 (1992).
[14]J. Phillips, S. Shim, I. M. Fonseca, and S. Carabineiro, Appl. Catal. **237**, 41 (2002).
[15]C. K. Chen, W. L. Perry, H. Xu, Y. Jiang, and J. Phillips, Carbon **41**, 2555 (2003).
[16]J. Phillips, C. C. Luhrs, and M. Richard, IEEE Trans. Plasma Sci. **37**(6) 726 (2009).
[17]T. N. Lambert, C. C. Luhrs, C. A. Chavez, S. Wakeland, M. T. Brumbach, and T. M. Alam, Carbon **48**, 4081 (2010).
[18]C. C. Luhrs, S. Wakeland, and B. Carpenter, "Graphene, graphitic and amorphous carbon nanostructures generation by atmospheric microwave plasma method," in *Plasma for Environmental Issues*, edited by E. Tatarova, V. Guerra, and E. Benova (Artgraf, Sofia, 2012)
[19]A. Dato, V. Radmilovic, Z. Lee, J. Phillips, and M. Frenklach, Nano Lett. **8**, 2012 (2008).
[20]E. Tatarova, J. P. Henriques, E. Felizardo, M. Lino da Silva, C. M. Ferreira, and B. Gordiets, J. Appl. Phys. **112**, 093301 (2012).
[21]E. Tatarova, F. M. Dias, J. P. Henriques, E. Felizardo, C. M. Ferreira, and B. Gordiets, Plasma Sources Sci. Technol. **17**, 024004 (2008).
[22]J. P. Henriques, E. Tatarova, F. M. Dias, and C. M. Ferreira, J. Appl. Phys. **109**, 023302 (2011).
[23]N. Bundaleska, D. Tsyganou, R. Saavedra, E. Tatarova, F. M. Dias, and C. M. Ferreira, Int. J. Hydrogen Energy **38**, 9145 (2013).
[24]M. Moisan and Z. Zakrzewski, J. Phys. D: Appl. Phys. **24**, 1025 (1991).
[25]J. Gonzalez-Aguilar, M. Moreno, and L. Fulcheri, J. Phys. D: Appl. Phys. **40**, 2361 (2007).
[26]M. Haruta and B. Delmon, J. Chim. Phys. Phys.-Chim. Biol. **83**, 859 (1986).
[27]A. C. Ferrari, J. C. Meyer, V. Scardaci, C. Casiragi, M. Lazzeri, F. Mauri, S. Piscanes, D. Jiang, K. S. Novoselov, S. Roth, and A. K. Geim, Phys. Rev. Lett. **97**, 187401 (2006).
[28]E. Tatarova, J. P. Henriques, F. M. Dias, and C. M. Ferreira, J. Phys. D: Appl. Phys. **39**, 2747 (2006).
[29]J. P. Henriques, E. Tatarova, F. M. Dias, and C. M. Ferreira, J. Appl. Phys. **103**, 103304 (2008).